Insulated gate bipolar transistor with trench gate structure of accumulation channel

Qian Mengliang(钱梦亮), Li Zehong(李泽宏)†, Zhang Bo(张波), and Li Zhaoji(李肇基)

(State Key Laboratory of Electronic Thin Films and Integrated Devices, University of Electronic Science and Technology, Chengdu 610054, China)

Abstract: An accumulation channel trench gate insulated gate bipolar transistor (ACT-IGBT) is proposed. The simulation results show that for a blocking capability of 1200 V, the on-state voltage drops of ACT-IGBT are 1.5 and 2 V at a temperature of 300 and 400 K, respectively, at a collector current density of 100 A/cm^2. In contrast, the on-state voltage drops of a conventional trench gate IGBT (CT-IGBT) are 1.7 and 2.4 V at a temperature of 300 and 400 K, respectively. Compared to the CT-IGBT, the ACT-IGBT has a lower on-state voltage drop and a larger forward bias safe operating area. Meanwhile, the forward blocking characteristics and turn-off performance of the ACT-IGBT are also analyzed.

Key words: ACT-IGBT; CT-IGBT; on-state voltage drop; forward blocking voltage; FBSOA
DOI: 10.1088/1674-4926/31/3/034002 **EEACC:** 2560

1. Introduction

So far, insulated gate bipolar transistors (IGBTs) have been the major switching device in power electronic applications as they have the merits of both power bipolar and power MOSFETs[1]. The planar-gate IGBT is gradually being replaced by the trench-gate IGBT (T-IGBT) which can provide a lower on-state voltage drop and higher latching current[2–4]. For a non-punch-through IGBT (NPT-IGBT), with the enhancement of blocking voltage, both the on-state voltage drop and on-state loss will increase. On the other hand, the latching current density of the conventional trench gate IGBT (CT-IGBT) decreases with increasing temperature, which hampers CT-IGBT from having wide applications in high temperature circumstances[5].

In this work, based on the planar accumulation channel field effect transistor structure proposed by Bobde and Baliga[6,7], we propose a novel ACT-IGBT. Using TSUPREM and MEDICI software, the forward breakdown voltage, on-state voltage drop, and FBSOA of the proposed device are investigated[8].

2. Device structure

Cross-sections of half-cells for the CT-IGBT and ACT-IGBT are shown in Figs. 1(a) and 1(b), respectively. From Fig. 1(b), we can see that the proposed ACT-IGBT structure eliminates the P base region in the CT-IGBT. In the ACT-IGBT, with a proper gap distance "L_0", the top N$^-$ base region near the emitter side is completely depleted due to the built-in potential of the P$^+$–N$^-$ junction. This creates a potential barrier to prevent the flow of electrons from the N$^+$ source to the N$^-$ base region[6,9]. As a result, the ACT-IGBT can support a higher forward blocking voltage with lower leakage current. The application of a positive bias to the gate will result in the formation of an accumulation layer, which provides a path for electrons to flow from the N$^+$ source to the N$^-$ base region. This yields a base drive current for the vertical P–N–P transistor in the ACT-IGBT structure, which promotes the injection of holes from backside P$^+$. Consequently, the ACT-IGBT can be operated with a lower on-state voltage drop because of the higher electron concentration in the accumulation layer near the emitter side.

3. Results and discussion

Unlike the conventional trench gate IGBT process, herein, the P base implantation and push in fabrication processes are eliminated. Prior to the emitter P$^+$ implantation process, emitter trench etching is performed during the ACT-IGBT process. A tilt of 7 degrees and energy of 100 keV are used for the P$^+$ implantation of the ACT-IGBT in this process. After being implanted, boron ions are activated by the subsequent BPSG reflow process for 20 min at 900 °C. The other processes for both structures are almost same, and some other important simulation parameters are listed in Table 1. The band-gap narrowing model "BGN", the Shockley–Read–Hall recombination model "SRH", the Auger recombination model "Auger", the concentration and temperature dependent mobility model

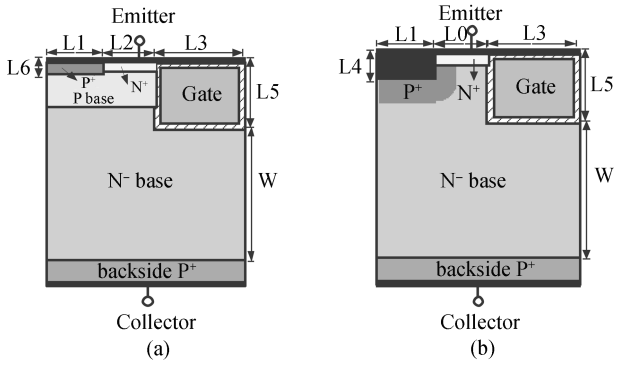

Fig. 1. (a) Cross-section of conventional CT-IGBT. (b) Cross-section of ACT-IGBT.

† Corresponding author. Email: lizh@uestc.edu.cn
Received 2 August 2009, revised manuscript received 15 October 2009

Table 1. Parameters for ACT-IGBT and CT-IGBT.

Denotation	Explanation	Value
L_0	Gap distance	1.5 μm
L_1	P^+ length in CT-IGBT	1.5 μm
L_2	N^+ emitter length in CT-IGBT	1.5 μm
L_3	Gate electrode length	1 μm
L_4	Emitter trench depth	2.5 μm
L_5	Trench gate depth	6 μm
L_6	N^+ emitter depth CT-IGBT	0.4 μm
W	Distance between gate and backside P+	169 μm
R	N^- base resistivity	55 Ω·cm
T_{ox}	Gate oxide thickness	62 nm
D_1	N^+ emitter (phosphorus) dosage	1×10^{16} cm^{-2}
D_2	P^+ (boron) dosage	1×10^{16} cm^{-2}
D_3	P base (boron) dosage	1×10^{14} cm^{-2}
D_4	Backside P^+ (boron) dosage	1×10^{14} cm^{-2}

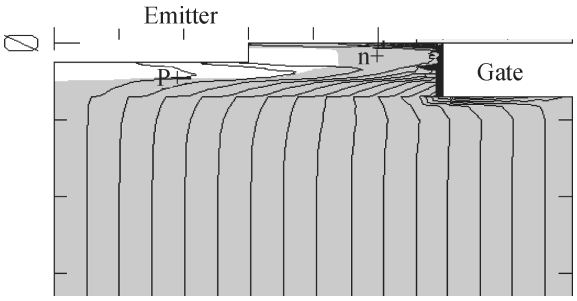

Fig. 2. Current flow lines of ACT-IGBT when V_{GE} and V_{CE} are 5 V.

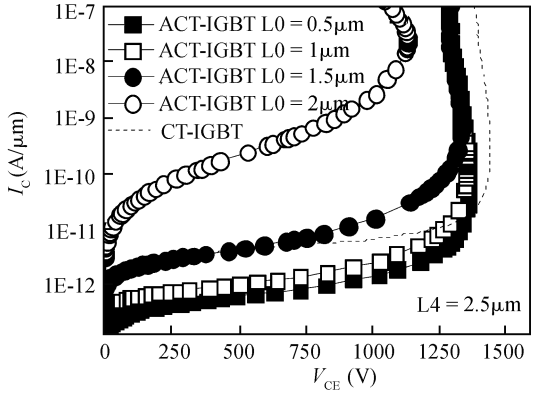

Fig. 3. Forward blocking characteristics of CT-IGBT and ACT-IGBT when L_4 is 2.5 μm.

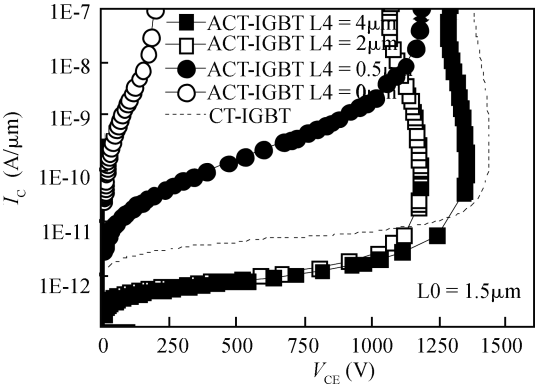

Fig. 4. Forward blocking characteristics of CT-IGBT and ACT-IGBT when L_0 is 1.5 μm.

"ANALYTIC", the electric field dependent model "PRPMOB" "FLDMOB" and the incomplete Choleski conjugate gradient method "ICCG" are applied to the simulation.

Both V_{GE} and V_{CE} are 5 V, and the current flow lines of the ACT-IGBT are shown in Fig. 2. While applying a positive gate bias of 5 V, an accumulation layer is formed along the trench sidewall. Therefore, electrons from the N^+ source flow into the N^- base region through this accumulation layer and serve as a base current of the vertical wide base PNP transistor. Holes are then injected from backside P^+ to modulate the N^- base region, and the rest of the holes are collected by the trench P^+ region at emitter as shown in Fig. 2. Thus, a higher latching current level can be acquired in the ACT-IGBT due to elimination of the P-base region of the CT-IGBT.

The gap distance L_0 as well as the emitter trench depth L_4 play an important role in determining the forward blocking characteristics of the ACT-IGBT. Figure 3 shows a comparison between the forward blocking characteristics of the CT-IGBT and the ACT-IGBT when the emitter trench depth L_4 is 2.5 μm. In Fig. 3, when L_0 is shorter than 1.5 μm, the ACT-IGBT can obtain as high a forward blocking voltage as CT-IGBT.

In contrast, for L_0 larger than 1.5 μm, the P^+ implanted in the trench is unable to deplete the N^- base completely with the built in potential, resulting in a high leakage current. The forward blocking characteristics of the CT-IGBT and the ACT-IGBT when the gap distance L_0 is 1.5 μm are shown in Fig. 4. From the figure, we know that the forward blocking voltage of the ACT-IGBT is proportional to the emitter trench depth L_4 when the gap distance L_0 is 1.5 μm. This is because that the electric field concentration at the corner of the trench bottom is relaxed due to the deeper emitter trench depth and the maximum electric field begins to shift from the corner of the trench bottom to the P^+ region as shown in Fig. 5. In addition, the ACT-IGBT with trench depth L_4 = 5 μm can obtain the same forward blocking voltage as the CT-IGBT, which is 1400 V, due to the electric field distribution by the deeper P^+ region as indicated in Fig. 5(c).

The potential barrier distribution of the CT-IGBT and the

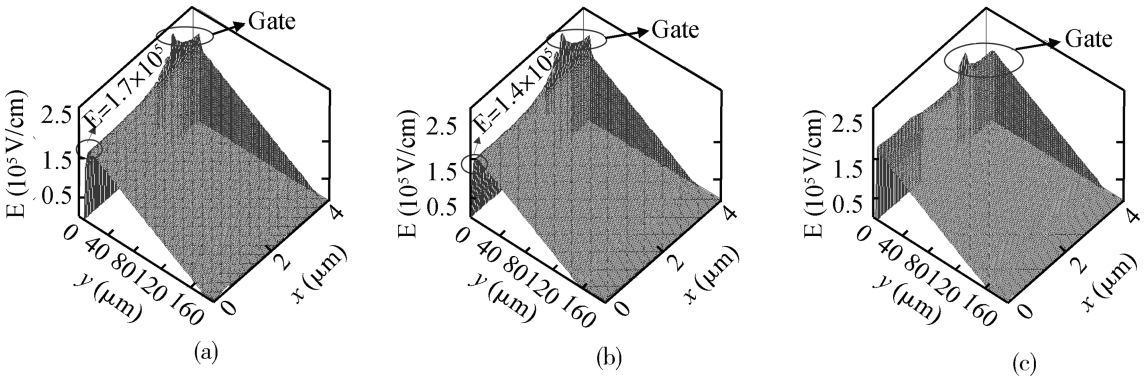

Fig. 5. 3-D E-field of (a) CT-IGBT, (b) ACT-IGBT with L_0 = 1.5 μm, L_4 = 0.5 μm, (c) ACT-IGBT with L_0 = 1.5 μm, L_4 = 5 μm.

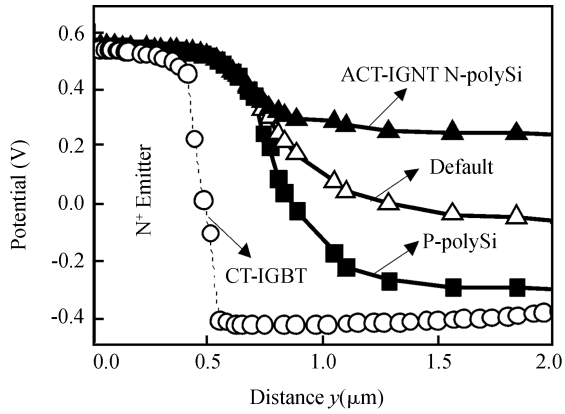

Fig. 6. Potential barrier distribution of CT-IGBT and ACT-IGBT along the channel region with V_{CE} = 0 V, V_G = 0 V (corresponding explanations in Fig. 5: "N-polySi" means N-type poly-silicon; "P-polySi" means P-type poly-silicon; "Default" means that boron-doped poly-silicon is used in the TSUPREM4 simulator and then the work function potential for the electrode is calculated from the doping in the MEDICI simulator).

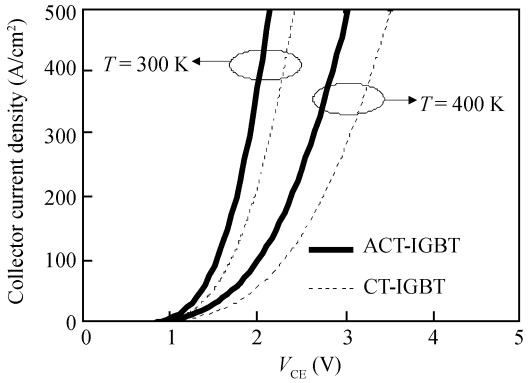

Fig. 7. On-state characteristics of CT-IGBT and ACT-IGBT at various temperatures (V_G = 15 V).

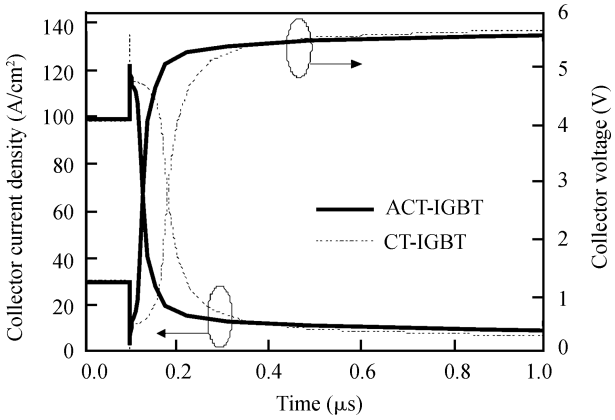

Fig. 8. Turn-off waveform of CT-IGBT and ACT-IGBT at a collector current density of 100 A/cm^2.

ACT-IGBT along the channel region (V_{CE} = 0 V, V_G = 0 V) is given in Fig. 6. As seen from Fig. 6, the CT-IGBT has a higher potential barrier than the ACT-IGBT. With an n-type poly-silicon gate, the potential barrier is much lower; an accumulation layer will be observed along the surface of the trench sidewall even at zero gate bias because the Fermi level in the n-type poly-silicon gate is higher than in the N^- base region. Therefore, a negative gate bias is needed when an n-type poly-silicon gate is used. The potential barrier can be increased by using P type poly-silicon, and the threshold voltage of P type poly-silicon can be increased from 0.7 V of the "default" mode to 1.1 V. The simulations done in this paper are based on the "default" mode.

It is worth mentioning that a positive charge in the gate oxide may cause a large ACT-IGBT leakage current, so P-type poly-silicon is essential for real fabrication, or a negative gate bias is preferred to ensure a low leakage current.

The on-state characteristics of the CT-IGBT and ACT-IGBT at different temperatures are shown in Fig. 7. This shows that the on-state voltage drops are 1.7 and 1.5 V for the CT-IGBT and ACT-IGBT, respectively, at an on-state current density of 100 A/cm^2 at 300 K. At a temperature of 400 K, the on-state voltage drops for the CT-IGBT and ACT-IGBT are 2.4 and 2 V, respectively. The improved on-state characteristic of the ACT-IGBT is attributed to the higher electron mobility and electron concentration in the accumulation channel.

Figure 8 shows the turn-off characteristics under resistive load conditions for the CT-IGBT and ACT-IGBT, when the turn-off time is approximately 0.4 μs for both devices. A minority carrier lifetime of 1 μs was fixed for the turn-off curves, which are simulated when the on-state current density at 100 A/cm^2 is turned off by removing the gate voltages of 15 and

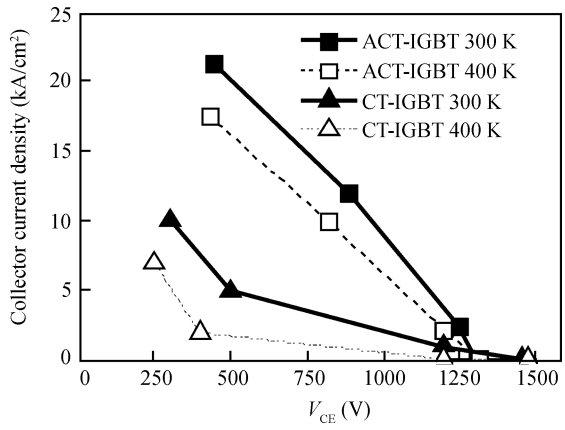

Fig. 9. FBSOA of CT-IGBT and ACT-IGBT at different temperatures.

5 V from the CT-IGBT and ACT-IGBT, respectively. The short turn-off time for the abrupt current drop of the ACT-IGBT observed in Fig. 8 is attributed to the carrier accumulation channel, which has a faster response rate to gate voltage.

The FBSOA of an IGBT is determined by the maximum voltage and current density that the device can operate without destructive failure at saturated collector current. Figure 9 shows the FBSOA of the CT-IGBT and ACT-IGBT at different temperatures. The ACT-IGBT has an increased FBSOA compared with the CT-IGBT at different operating temperatures. It is obvious in Fig. 9 that the ACT-IGBT can operate without destructive failure with a collector voltage of 447 V and a current density of 21200 A/cm^2 at an operating temperature of 300 K. It can be seen that a current density of 10 kA/cm^2 can be saturated up to 820 V even at an operating temperature of 400 K. Consequently, the FBSOA of the ACT-IGBT is considerably wider than that of the CT-IGBT over the total operating temperature range.

4. Conclusion

A novel trench-gate insulated gate bipolar transistor with accumulation channel is described. A numerical simulation of the conventional trench-gate IGBT and ACT-IGBT is carried out. The results show that the accumulation channel is very effective in reducing the on-state voltage drop. The elimination of the P base region in the CT-IGBT is beneficial for increasing the latching current of the ACT-IGBT, and thus a larger FBSOA can be acquired. In addition, the ACT-IGBT can provide improved forward blocking characteristics with an appropriate design.

References

[1] Lorenz L. Power semiconductor devices development trends and system interactions. PCC, 2007: 348
[2] Nemoto M, Baliga B J. The recessed-gate IGBT structure. ISPSD, 1999: 149
[3] Khanna V K. The insulated gate bipolar transistor (IGBT) theory and design. 1st ed. Canada: Institute of Electrical and Electronics Engineers, 2003
[4] Udrea F, Amaratunga G A K. Theoretical and numerical comparison between DMOS and trench technologies for insulated gate bipolar transistors. IEEE Trans Electron Devices, 1995, 42: 1356
[5] Baliga B J. Power semiconductor devices. Boston: PWS Publishing Co, 1996
[6] Bobde M D, Baliga B J. Silicon planar ACCUFET improved power MOSFET structure. Electron Lett, 2000, 36: 913
[7] Baliga B J. The future of power semiconductor device technology. Proc IEEE, 2001, 89: 822
[8] Medici User's Manual. Avant! Corporation. 2004
[9] Li Zehong, Qian Mengliang, Zhang Bo. TAC IGBT: an improved IGBT structure. ISPSD, 2009: 124